All-Order Polarization-Mode-Dispersion (PMD) Compensation at 40 Gb/s via Hyperfine Resolution Optical Pulse Shaping

Li Xu, Houxun Miao, and A. M. Weiner, *Fellow, IEEE*

***Abstract*—For the first time, we report lightwave system experiments testing a concept for all-order polarization-mode-dispersion (PMD) compensation based on optical pulse shaping. Our results demonstrate compensation of PMD with $>$50-ps average differential group delay, well into the all-order regime, in a 40-Gb/s return-to-zero ON–OFF keying experiment.**

***Index Terms*—Fiber-optics communications, fiber-optics components, fiber-optics sensors, polarization.**

I. INTRODUCTION

POLARIZATION-MODE dispersion (PMD) [1] is considered a major obstacle for ultrahigh-capacity fiber communication systems at 40 Gbaud/s and above. Although some electrical PMD compensation (PMDC) is possible, it is complex and expensive for high symbol rates, and to date experiments reaching to 40 Gbaud/s are limited. Furthermore, most research on PMDC, either electrical or optical, has been limited to the first- or second-order PMD regime, valid only for distortions which are small compared to the bit period or pulsewidth. Our group has previously demonstrated optical compensation of all-order PMD by using a novel optical pulse shaping approach [2], [3]. In this previous work, the compensator was tested with low repetition rate, isolated pulses. In [2], pulses were distorted and spread over $>$100 ps as a result of all-order PMD, then successfully restored via PMDC to their original 15-ps duration; whereas in [3], 800-fs pulses were fully compensated after being distorted to $>$10 ps by all-order PMD. Here for the first time we demonstrate such all-order PMDC in a lightwave system experiment at 40 Gbaud/s (realized via 10 Gb/s $\times$ 4 optical time-division multiplexing (OTDM) for compatibility with the speed of our bit-error-rate (BER) tester). We report successful compensation for PMD with average differential group delay (DGD) (i.e., DGD averaged over optical frequency) of more than 50 ps, twice the symbol period and well into the all-order regime. Our results show the possibility of compensating PMD distortion effects so large that they are usually viewed as intractable. Furthermore, since our pulse shaping approach has been demonstrated to scale to pulses in the subpicosecond regime [3], our results hold promise for application to much higher bit rate systems where strong PMD effects are increasingly likely to occur.

Manuscript received March 03, 2010; revised April 21, 2010; accepted April 25, 2010. Date of publication May 17, 2010; date of current version June 30, 2010. This work was supported by the National Science Foundation under Grant ECS-0501366.

L. Xu and A. M. Weiner are with the Department of Electrical and Computer Engineering, Purdue University, West Lafayette, IN 47907-2035 USA (e-mail: xu36@purdue.edu; amw@purdue.edu).

H. Miao was with the Department of Electrical and Computer Engineering, Purdue University, West Lafayette, IN 47907-2035, USA. He is now with the Center for Nanoscale Science and Technology, National Institute of Standards and Technology, Gaithersburg, MD 20899-6203 USA (e-mail: houxun.miao@nist.gov).

Digital Object Identifier 10.1109/LPT.2010.2049647

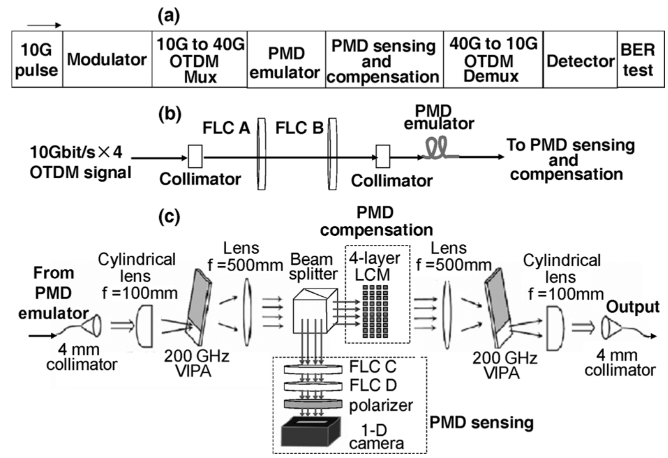

Fig. 1. Experimental setup: (a) the whole setup; (b) PMD emulator; (c) PMD sensing and compensation.

II. EXPERIMENTAL SETUP AND METHOD

As shown in Fig. 1(a), our experimental setup includes a transmitter, a PMD emulator, and a receiver. The transmitter comprises a 10-GHz short pulse source, a modulator, and an optical 10- to 40-G OTDM multiplexer. The receiver includes PMD sensing optics and the PMD compensator, a 40- to 10-G OTDM demultiplexer, a 10-GHz photodiode, and a BER test set.

The pulse source starts with a continuous-wave (CW) laser, which is strongly modulated at 10 GHz to form a comb, then phase compensated via a pulse shaper to generate $\sim$3-ps full-width at half-maximum (FWHM) pulses [4]. Amplification and adiabatic soliton compression in a dispersion decreasing fiber generates a broad flat spectrum from which we slice a smooth spectrum of $\sim$120-GHz bandwidth FWHM [Fig. 2(a)]. For modulation, we use both 10-Gb/s ON–OFF keying intensity modulation and pseudorandom 0-π phase modulation for carrier suppression. The smooth spectrum resulting from carrier suppression, shown in Fig. 2(b), is more favorable for spectral polarimetry which we use in our PMD sensing scheme. The autocorrelation of the 10-Gb/s signal without PMD is shown in Fig. 2(c), from which we estimate a pulse duration of 5.9-ps

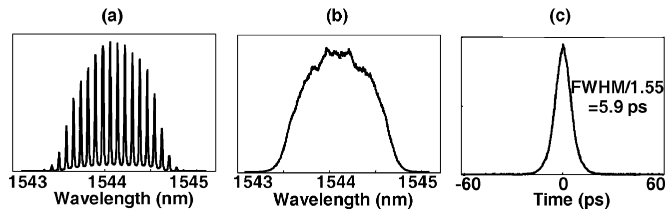

Fig. 2. (a) Spectrum of 10-G short pulse; (b) spectrum of one 10-Gb/s channel with intensity modulation and carrier-suppression; (c) autocorrelation measurement of 10-Gb/s signal after it goes through PMDC module back-to-back.

FWHM. The 10- to 40-G OTDM multiplexer generates four decorrelated channels from the original 10-Gb/s pulses. All channels have the same state of polarization (SOP) before going to the PMD emulator. The homemade PMD emulator is the concatenation of over 10 polarization-maintaining fiber sections with randomly set fast axes and different lengths. As shown in Fig. 1(b), two ferroelectric liquid crystal (FLC) cells are used to impose a sequence of four different polarization transformations onto the signal prior to the emulator, which is used to sense the frequency-dependent Jones matrix of the PMD [2], [3], [5]. The PMD sensing and compensation module (with 19-dB loss) is shown in Fig. 1(c). The spectrum of the input signal is dispersed in free space by a virtually imaged phase array (VIPA) [6] with 200-GHz free spectral range. The chromatic dispersion of the apparatus is minimized by appropriately setting the VIPA-lens separations. A polarization-insensitive beam splitter directs a portion of the signal to our fast wavelength-parallel polarimeter [5], with the remaining signal going to a 128-pixel $\times$ 4-layer liquid crystal modular (LCM) array for PMDC [2], [3]. Each LCM pixel has $> 2\pi$ retardation range with tens of ms response time. All retardation values are programmed modulo 2π to fit within a 2π range. The spectral dispersion across the pixels of the LCM array and of the one-dimensional camera (used in PMD sensing) are carefully matched, with a value of 1.6 GHz/pixel. By sequentially transforming the launch polarization into the PMD emulator and measuring the frequency-dependent polarization of the output light for each launch, we are able to calculate the frequency-dependent Jones matrix of the emulator at each frequency sample. In the compensation process the first three layers of the LCM array are programmed to generate the inverse frequency-dependent Jones matrix. The third and fourth layers also compensate isotropic spectral phase (equivalent to generalized or high-order chromatic dispersion) introduced by the PMDC step. This combination realizes complete all-order PMDC. The home-made optical 40- to 10-G OTDM demultiplexer, realized by cascading two 10-GHz intensity modulator, gives a timing gate of 16.5-ps FWHM.

When we perform a back-to-back system BER test, first we let the signal pass the whole system except PMD emulator and PMDC module. In BER test results, there is 1.7-dB power penalty for one channel demuxed from 10 Gb/s $\times$ 4 OTDM signal compared with BER of the original 10-Gb/s signal. Then we let the signal go through the whole system without PMD emulator but with PMDC module (set for a quiescent state). The BER result shows 1 dB more power penalty (2.7 dB in total), which is caused by 10% spectrum narrowing introduced by VIPA passband. We use the latter back-to-back BER result

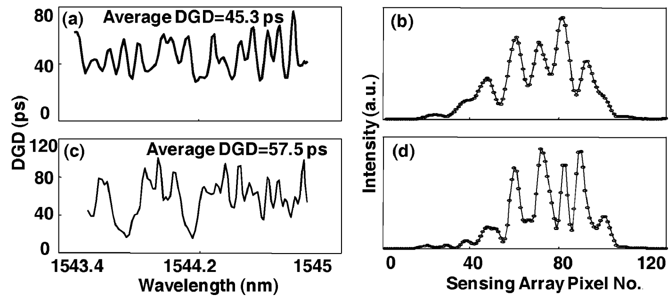

Fig. 3. (a), (c) DGD versus wavelength and (b), (d) representative results from the SOP sensing measurements for (a), (b) first and (c), (d) second PMD emulator, respectively. For (b), (d) we show the intensity of the 0° linear polarization component versus pixel number (frequency) for a particular launch polarization into the emulator.

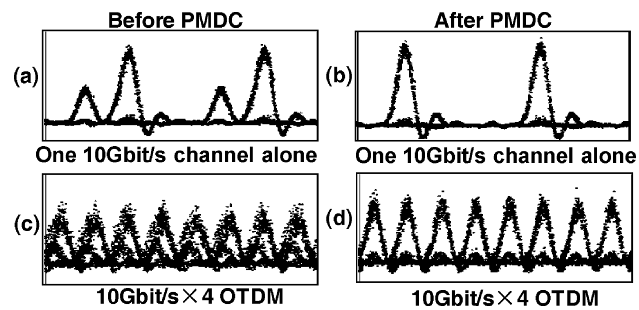

Fig. 4. Eye diagrams (200-ps time range) before and after PMDC for the emulator with 45.3-ps average DGD.

as our baseline to estimate the quality of PMDC after a PMD emulator is inserted.

III. Experimental Results

In the following we report PMDC results for two emulators with average DGD of (Case 1) 45.3 ps and (Case 2) 57.5 ps. DGD versus wavelength data are shown in Fig. 3(a) and (c), derived from our wavelength-parallel Jones matrix measurements [5]. In both cases, the DGD takes on values which are quite large compared to the 5.9-ps pulsewidth and the 25-ps symbol period. This puts us well into the regime where Taylor series approximations to the PMD break down and all-order PMD must be considered.

In both cases, a 50-GHz photodiode is used before the 40- to 10-G demultiplexer to measure eye diagrams, both with and without PMDC. Results are shown both for a single 10-Gb/s input channel and for the 10 Gb/s $\times$ 4 OTDM signal. A 10-G photodiode is used to measure BERs after a single 10-G channel is demuxed from the four OTDM channels.

The PMDC results for Case 1 are shown in Fig. 4. For this emulator, DGD versus wavelength varies over a 30- to 80-ps range with 45.3-ps average value. This broadens and distorts the 10-Gb/s signal, Fig. 4(a). For 10 Gb/s $\times$ 4 OTDM, Fig. 4(c), strong intersymbol interference (ISI) degrades the eye. The BER for a single channel after demux is very poor ($\sim 0.2-0.4$). After PMDC, the 10-G pulse is compensated to its original shape, Fig. 4(b), and clean eyes are recovered for 40-Gb/s operation, Fig. 4(d). From Fig. 6, the BER is improved significantly after PMDC. Although there is a 2.5-dB power penalty, error rates down to a few times 10^{-9} are obtained.

Results for Case 2 are shown in Fig. 5. Here the DGD versus wavelength varies between 10 and 100 ps, with 57.5-ps average

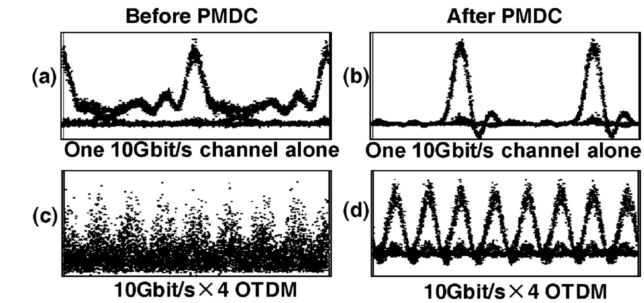

Fig. 5. Eye diagrams (200-ps time range) before and after PMDC.

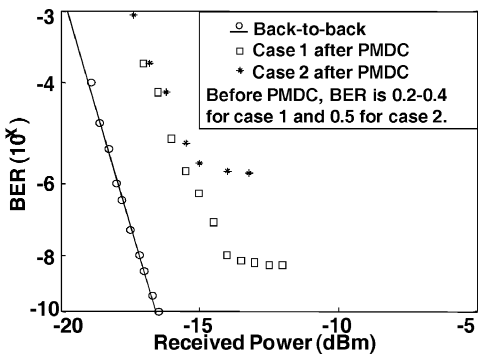

Fig. 6. BER after PMDC for Case 1 (45.3-ps average DGD) and Case 2 (57.5-ps average DGD). BERs without PMDC are not plotted.

DGD, as in Fig. 3(c). The original 5.9-ps pulse is broadened to approximately the 100-ps range. For 10 Gb/s $\times$ 4 OTDM in Fig. 5(c), the ISI is so strong that the eyes completely close, and the BER is essentially 0.5. After PMDC, the 10-G pulse is compensated to its original shape, and clean eyes are recovered for the 40-G signal, Fig. 5(b) and (d). From Fig. 6, the BER goes down to a floor of $\sim 10^{-6}$, well into the range in which FEC is possible, with $\sim$3-dB power penalty compared to back-to-back.

Although substantial PMDC is achieved, it is also clear that some degradation remains. We attribute this to limited spectral resolution, both in sensing and compensation. Although the spectrum is dispersed to 1.6 GHz/pixel, the actual beam size for any single frequency covers two pixels, for $\sim$3-GHz resolution. When PMD is large, SOP varies very rapidly with frequency. In Fig. 3(b) and (d), we show measured intensity versus pixel for our polarization sensor for the 0° linear SOP component. Finer features are observed as the average DGD increases. For example, for Fig. 3(d), the feature near pixel 80 is only three pixels wide. Such features approach the spectral resolution limit of our apparatus and introduce inaccuracy. The ability of the compensation module to control the frequency-dependent Jones matrix is limited by the same spectral resolution limits. Although the PMDC data for individual 10-Gb/s channels looks OK, spectral resolution issues contribute to slight reshaping of our pulses, which as a result no longer fully conform to the strict interferometric crosstalk requirements in OTDM systems [7].

In the figures above, the eye diagrams are taken when the polarization switching used for PMD sensing is switched OFF. For Fig. 7(b), we continuously switch between two polarization states at 2-kHz frequency during the PMDC operation (using the Case 1 emulator). As in previous isolated pulse experiments [2], polarization switching does not significantly affect the recovered pulse compared with Fig. 7(a) which is without switching. This provides evidence that the in-line polarization switching we use at the input, in order to allow real-time Jones matrix sensing, is compatible with simultaneous data transmission.

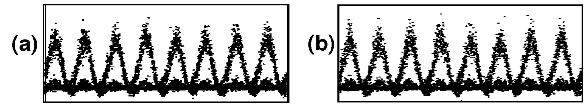

Fig. 7. Eye diagrams (200-ps time range) of 10 Gb/s $\times$ 4 OTDM. after PMDC. (a) With fixed input SOP to PMD emulator; (b) with input SOP to PMD emulator switching at 2 kHz between 0° and 90° linear SOP.

IV. Conclusion

We experimentally demonstrate feed-forward all-order optical PMDC in a 10 Gb/s $\times$ 4 OTDM system with very large PMD (average DGD $>$ 50 ps) using a hyperfine resolution pulse shaper provisioned with a four-layer liquid crystal modulator array and frequency-dependent Jones matrix sensing. This shows the possibility of PMDC at 40-Gbaud symbol rate for distortions so large their compensation is usually viewed as intractable. Furthermore, our all-optical approach can readily be extended to higher symbol rates (pulses down to the subpicosecond range [3]). It is important to note that our compensation system is essentially static and does not address rapid dynamic effects such as cross-polarization modulation in wavelength-division multiplexing systems. Furthermore, polarization-dependent loss is not considered in the current work and remains a topic for future investigation.

Acknowledgment

The authors acknowledge D. Leaird for discussions and technical assistance and Avanex Corp. for donating the VIPA.

References

[1] H. Kogelnik, R. M. Jopson, and L. E. Nelson, “Polarization mode dispersion,” in *Optical Fiber Telecommunications IVB-Systems and Impairments*, I. P. Kaminow and T. Li, Eds. New York: Academic, 2002.

[2] H. X. Miao, A. M. Weiner, L. Mirkin, and P. J. Miller, “All-order polarization-mode dispersion (PMD) compensation via virtually imaged phase array (VIPA)-based pulse shaper,” *IEEE Photon. Technol. Lett.*, vol. 20, no. 8, pp. 545–547, Apr. 15, 2008.

[3] H. X. Miao, A. M. Weiner, L. Mirkin, and P. J. Miller, “Broadband all-order polarization mode dispersion compensation via wavelength-by-wavelength Jones matrix correction,” *Opt. Lett.*, vol. 32, pp. 2360–2362, Aug. 2007.

[4] C.-B. Huang, Z. Jiang, D. E. Leaird, and A. M. Weiner, “High-rate femtosecond pulse generation via line-by-line processing of a phase-modulated CW laser frequency comb,” *Electron. Lett.*, vol. 42, pp. 1114–1115, Sep. 2006.

[5] L. Xu, S. X. Wang, H. Miao, and A. M. Weiner, “Polarization mode dispersion spectrum measurement via high-speed wavelength-parallel polarimetry,” *Appl. Opt.*, vol. 48, no. 24, pp. 4688–4697, 2009.

[6] M. Shirasaki, “Large angular dispersion by a virtually imaged phased array and its application to a wavelength demultiplexer,” *Opt. Lett.*, vol. 21, pp. 366–368, Mar. 1996.

[7] A. T. Poulsen *et al.*, “Pulse source requirements for OTDM systems,” in *Proc. LEOS*, 2003, vol. 1, pp. 382–383.